A Ssd1 homolog impacts trehalose and chitin biosynthesis and contributes to virulence in *Aspergillus fumigatus*

Running Title: Ssd1 homolog impacts *Aspergillus* cell wall

Arsa Thammahong[1,*a], Sourabh Dhingra[1], Katherine M. Bultman[1,*b], Joshua Kerkaert[1], Robert A. Cramer[1#]

[1] Department of Microbiology and Immunology, Geisel School of Medicine at Dartmouth, Hanover, New Hampshire, United States of America

[*a] Current Address: Antimicrobial Resistance and Stewardship Research Unit, Department of Microbiology, Faculty of Medicine, Chulalongkorn University, Bangkok, Thailand

[*b] Current Address: Microbiology Doctoral Training Program, University of Wisconsin Madison, Madison, Wisconsin, United States of America

Corresponding author

E-mail: Robert.A.Cramer.Jr@dartmouth.edu (RAC)

Abstract Word Count: **185**

Manuscript Word Count: **3575**

Abstract

Regulation of fungal cell wall biosynthesis is critical to maintain cell wall integrity in the face of dynamic fungal infection microenvironments. In this study, we observe that a yeast *ssd1* homolog, *ssdA*, in the filamentous fungus *Aspergillus fumigatus* is involved in trehalose and cell wall homeostasis. An *ssdA* null mutant strain exhibited an increase in trehalose levels and a reduction in colony growth rate. Over-expression of *ssdA* in contrast perturbed trehalose biosynthesis and reduced conidia germination rates. The *ssdA* null mutant strain was more resistant to cell wall perturbing agents while over-expression of *ssdA* promoted increased sensitivity. Over-expression of *ssdA* significantly increased chitin levels and both loss and over-expression of *ssdA* altered sub-cellular localization of the class V chitin synthase CsmA. Strikingly, over-expression of *ssdA* abolished adherence to abiotic surfaces and severely attenuated the virulence of *A. fumigatus* in a murine model of invasive pulmonary aspergillosis. In contrast, despite the severe *in vitro* fitness defects observed upon loss of *ssdA*, neither surface adherence or murine survival was impacted. In conclusion, *A. fumigatus* SsdA plays a critical role in cell wall homeostasis that alters fungal-host interactions.

Importance

Life threatening infections caused by the filamentous fungus *Aspergillus fumigatus* are increasing along with a rise in fungal strains resistant to contemporary antifungal therapies. The fungal cell wall and the associated carbohydrates required for its synthesis and maintenance are attractive drug targets given that many genes encoding proteins involved in cell wall biosynthesis and integrity are absent in humans. Importantly, genes and associated cell wall biosynthesis and homeostasis regulatory pathways remain to be fully defined in *A. fumigatus*. In this study, we identify SsdA, a model yeast Ssd1p homolog, as an important component of trehalose and fungal cell wall biosynthesis in *A. fumigatus* that consequently impacts fungal virulence in animal models of infection.

Introduction

Aspergillus fumigatus is the most common filamentous fungus that causes a wide variety of human diseases ranging from allergic type diseases to acute invasive infections. Invasive aspergillosis (IA) in immune compromised hosts, e.g. patients with hematological malignancies and organ or stem cell transplant recipients is associated with high mortality (1). Antifungal drugs used to treat IA, e.g. voriconazole, amphotericin B, are associated with undesired side effects, detrimental drug-drug interactions, long therapeutic regimens, and persistence of poor patient outcomes (2-5). To compound the difficulty of treating these infections, the emergence of azole-resistant *Aspergillus* infections is increasing globally (6-28). In order to make therapeutic advances against these increasingly common and potentially drug resistant infections, new antifungal drugs are needed.

One existing antifungal drug target that has not been fully exploited is the fungal cell wall. Consisting mainly of polysaccharides including β-1,3-glucans, alpha-glucans, mannan, chitin, and galactosaminogalactan among others (29-38), the cell wall is a great antifungal drug target as evidenced by the development of the echinocandins that target β-1,3-glucan biosynthesis. Interestingly, the carbohydrates needed to generate β-1,3-glucan and chitin, i.e. glucose 6-phosphate and UDP-glucose, are also important substrates used to generate trehalose, a disaccharide sugar, that is important for fungal conidia germination, stress protection, cell wall homeostasis, and virulence (39, 40). The canonical trehalose biosynthesis pathway in *A. fumigatus* consists of two enzymes, TpsA/B (trehalose-6-phosphate synthase) and OrlA (trehalose-6-phosphate phosphatase), and two regulatory-like subunits, TslA and TslB (39-41). Trehalose biosynthesis is also found in other organisms in addition to fungi including bacteria, plants, and insects, but is not found in humans (42).

We and others previously observed that proteins involved in trehalose biosynthesis impact cell wall homeostasis in *A. fumigatus* (39-41). Disruption of the trehalose-6-phosphate

phosphatase, OrlA, leads to perturbations in cell wall integrity as observed by the increased sensitivity to the cell wall perturbing agents congo red, calcofluor white, and nikkomycin Z (40). Loss of OrlA attenuates virulence of *A. fumigatus* in chronic granulomatous disease (xCGD) and chemotherapeutic invasive pulmonary aspergillosis (IPA) murine models. In addition, a regulatory subunit of the trehalose biosynthesis pathway, TslA, is critical for trehalose production and cell wall homeostasis in part through regulation of a class V chitin synthase enzyme, ChsE/CsmA (41). Loss of TslA increased chitin production and altered the sub-cellular localization of CsmA (41). Pulldown assays with TslA as bait identified a physical interaction between TslA and CsmA as well as a putative *Saccharomyces cerevisiae* Ssd1 homolog, herein called SsdA.

Ssd1p is a pleiotropic RNA-binding protein (43, 44) that is important for chromosome stability at high temperature, vesicular trafficking, stress responses, and cell wall integrity in *S. cerevisiae* (45-49). Ssd1p genetically interacts with Pkc1p and Sit4p, which are important components of the cell wall integrity signaling pathway (48). It has been shown that *S. cerevisiae ssd1* null mutants isolated from both patients and plants are more virulent than wild type strains in a DBA/2 murine model (50). Similar to the *A. fumigatus tslA* null mutant, the cell wall composition of yeast *ssd1* null mutants contain more chitin and mannan with decreases in β-1,3-glucan and β-1,6-glucan (50). These cell wall changes lead to increased proinflammatory responses against *ssd1* mutant strains (50). In contrast to *S. cerevisiae*, the *ssdA/ssdA* null mutant in *C. albicans* has decreased virulence in the invasive systemic candidiasis murine model (51). In filamentous fungal pathogens, the function of Ssd1 homologs is less clear, but in the plant pathogen *Magnaporthe grisea*, *SSD1* is important for fungal colonization of rice leaves (52). The authors suggested that *SSD1* is essential for proper cell wall assembly leading to evasion of the host immune response (52). However, the mechanism(s) behind this phenotype is not well understood (52). In this study, we

characterized a predicted Ssd1p homolog identified in *A. fumigatus* through its protein-protein interaction with the trehalose biosynthesis protein, TslA. Using a genetics approach, we observe that *A. fumigatus* SsdA is critical for cell wall biosynthesis, trehalose production, polarized growth, biofilm formation, and virulence of *A. fumigatus*. Our results support the known role of Ssd1 homologs in fungal cell wall biosynthesis and highlight the potential altered functions of *A. fumigatus ssdA* including those involved in trehalose biosynthesis, biofilm formation, and fungal virulence.

Results

SsdA regulates trehalose production and is required for *Aspergillus fumigatus* conidia germination and mycelium expansion

AFUB_010850 was identified in a mass-spectrometry based screen of proteins that interact with the trehalose biosynthesis regulatory protein, TslA (41). Protein domain analysis of AFUB_010850 revealed strong amino acid sequence similarity with the nucleic acid binding Interpro domain IPR012340 ($5.0E^{-109}$) and the ribonuclease (RNB) PFAM domain PF00773 ($4.4E^{-88}$). BLASTP analysis of the AFUB_010850 amino acid sequence against the *Saccharomyces cerevisiae* genome database revealed strong sequence similarity to the protein SSD1p. Consequently, reciprocal BLASTP analyses with SSD1p against the *A. fumigatus* genome suggested AFUB_010850 is likely an Ssd1p ortholog and hence we named AFUB_010850 *ssdA*. Given the previously identified roles of TslA in trehalose and cell wall homeostasis in *A. fumigatus,* and the known roles of *ssd1* homologs in fungal cell wall biosynthesis, we hypothesized that SsdA is an important mediator of trehalose production and cell wall homeostasis in *A. fumigatus*.

To test this hypothesis, we generated *ssdA* null mutant (Δ*ssdA)* and over-expression strains (OE:*ssdA)* (confirmed by PCR and Southern blot analyses). The *ssdA* null mutant was

complemented with an *ssdA:GFP* allele. We next measured the trehalose content of both conidia and mycelia in the respective strains (53). We observed increased trehalose content in Δ*ssdA* conidia and mycelia and conversely reduced trehalose levels in OE:*ssdA* (P=0.0004, compared Δ*ssdA* to the wild type; P<0.0001 compared OE:*ssdA* to the wild type) **(Fig. 1A)**. Reconstitution of Δ*ssdA* with *ssdA:GFP* restored wild-type trehalose levels. These data suggest that SsdA plays a role in regulating trehalose biosynthesis and/or levels in *A. fumigatus*.

To determine if *ssdA* plays a role in conidia germination and polarized growth, we measured radial growth of the respective strains' fungal mycelium on solid medium (**Fig. 1B, C**) and liquid planktonic culture biomass (**Fig. 1D**) in 1% glucose minimal medium (GMM). We observed that on solid GMM both the Δ*ssdA* and OE:*ssdA* strains exhibited decreased mycelial radial growth after a 72-hour incubation at 37°C compared to the wild type and reconstituted strains (Δ*ssdA*+*ssdA:GFP*) (P<0.0001 Δ*ssdA* to the wild type and P=0.0001 OE:*ssdA* to the wild type) (**Fig. 1B, C**). In planktonic liquid cultures, 24-hour biomass from Δ*ssdA* and OE:*ssdA* cultures grown at 37°C was reduced compared to the wild-type and reconstituted strains (P=0.0133 Δ*ssdA* to the wild type and P=0.0023 OE:*ssdA* to the wild type) (**Fig. 1D**). Δ*ssdA* conidia germinated faster in the first 6-8 hours (P<0.01, Δ*ssdA* to the wild type) while OE:*ssdA* conidia germinated slower during the first 12 hours and then caught up to the wild type at 24 hours (P<0.0001, OE:*ssdA* to the wild type) (**Fig. 1E**). The reduced germination observed in OE:*ssdA* conidia is consistent with the reduction in trehalose levels in these fungal cells as Al-Bader, *et al.* observed that depletion of trehalose content in an *A. fumigatus tpsA/tpsB* double null mutant deficient in trehalose delayed conidia germination (39). However, *A. fumigatus* trehalose mutants do not have *in vitro* growth defects when glucose is the primary carbon source and we cannot attribute *ssdA* mutant growth defects to alterations in trehalose levels. Taken together, these results implicate SsdA

in trehalose biosynthesis and support a global role for SsdA in fungal fitness when glucose is the sole carbon source.

SsdA is important for cell wall integrity

A. fumigatus trehalose null mutants including Δ*tslA* have altered cell wall integrity and previous research identified a link between yeast Ssd1p and *Neurospora crassa* GUL-1 (SSD1 homolog) function and the cell wall (39, 40, 50, 54). We next utilized the cell wall perturbing agents congo red (1 mg/mL), calcofluor white (CFW, 50 μg/mL), and the echinocandin caspofungin (2 μg/mL) to test the hypothesis that *A. fumigatus* SsdA is important for cell wall integrity. Δ*ssdA* exhibited increased resistance to cell wall perturbing agents while OE:*ssdA* exhibited increased susceptibility, particularly to congo red and calcofluor white **(Fig. 2)**.

We hypothesized that the altered growth and change in susceptibility to cell wall perturbing agents observed in SsdA mutants comes from altered cell wall composition and/or organization. To initially test this hypothesis, CFW and wheat germ agglutinin (WGA) were used to interrogate total and exposed chitin respectively, while soluble human dectin-1-FC was used to examine β-1,3-glucan exposure. We observed a large decrease in the intensity of CFW and WGA staining of Δ*ssdA* germlings while in contrast germlings of OE:*ssdA* showed increased intensity with these chitin binding molecules (P=0.0322, Δ*ssdA* to the wild type, P<0.0001, OE:*ssdA* to the wild type) (**Fig. 3A**). For β-1,3-glucan, we observed a decrease in soluble dectin1-FC staining on both the Δ*ssdA* and the OE:*ssdA* germlings suggestive of a decrease in β-1,3-glucan exposure (P=0.0389, Δ*ssdA* to the wild type, P<0.0001, OE:*ssdA* to the wild type) (**Fig. 3**). While additional quantitative cell wall composition analyses are needed, these data support the hypothesis that SsdA impacts *A. fumigatus* cell wall integrity.

198 Given the changes in the cell wall of the Δ*ssdA* and the OE:*ssdA* strains, we next
199 tested their ability to adhere to an abiotic surface. Using the crystal violet adherence assay,
200 we observed no difference in adherence between the wild-type, Δ*ssdA*, and reconstituted
201 strains. However, a striking loss of adherence was observed in the OE:*ssdA* strain **(Fig. 4A).**
202 To investigate this adherence difference further, spinning disk confocal microscopy, in
203 combination with the galactosaminogalactan binding FITC labeled soy bean agglutinin
204 (SBA), was utilized. Given the decreased adherence of the overexpression strain, we were
205 surprised that increased expression of *ssdA* resulted in much greater levels of SBA staining,
206 revealing striking differences compared to the wild-type and Δ*ssdA* strains **(Fig. 4B).** As SBA
207 binds to oligosaccharides with alpha- or beta-linked N-acetylgalactosamine and, to a lesser
208 extent, galactose residues, we tested whether mRNA levels of the UDP-glucose 4-epimerase
209 involved in galactosaminogalactan biosynthesis were altered in the *ssdA* mutant strains (55).
210 No significant difference in *uge3* mRNA levels were observed under the conditions
211 examined, suggesting a role for *ssdA* in post-transcriptional regulation of the
212 galactosaminogalactan polysaccharide (**Fig. 4C).** Taken together, these data suggest that *ssdA*
213 expression levels impact fungal adherence.
214 Given the responses of the *ssdA* mutant strains to agents and reagents that inhibit or
215 bind to chitin, a non-radioactive chitin synthase activity assay was next utilized to further
216 define the impact of SsdA levels on the *A. fumigatus* cell wall (56, 57). Consistent with the
217 cell wall immunohistochemistry results, chitin synthase activity in Δ*ssdA* was significantly
218 reduced while in contrast chitin synthase activity in OE:*ssdA* was significantly increased
219 (P=0.0029, Δ*csmA* to the wild type; P=0.0208, Δ*ssdA* to the wild type; P<0.0001, OE:*ssdA*
220 to the wild type) (**Fig. 5A**). We previously observed that activity and localization of the chitin
221 synthase CsmA was perturbed by loss of the trehalose regulatory protein TslA (41). As TslA

was found to also physically interact with SsdA, we hypothesized that SsdA levels may also impact CsmA sub-cellular localization.

To study CsmA sub-cellular localization when SsdA levels are altered, we introduced a C-terminal GFP-tagged *csmA* allele into the respective *ssdA* mutant strains. Using spinning disk confocal microscopy, we observed that alteration of *ssdA* mRNA levels (loss or increase) led to an altered CsmA localization pattern compared to the wild-type and reconstituted strains (**Fig. 5B**). CsmA:GFP puncta observed in Δ*ssdA* are mainly focused at the hyphal tip with a few puncta also localized along the lateral hyphal walls but no visible localization at the conidial septum. In contrast, in OE:*ssdA* CsmA:GFP puncta were dispersed throughout the hyphae with no visible puncta at the hyphal tip or conidial septum (**Fig. 5B**). Intriguingly, this latter result is similar to the diffuse sub-cellular localization of CsmA:GFP in the absence of TslA (41). Taken together, these results suggest SsdA levels affect sub-cellular localization of the chitin synthase CsmA.

SsdA levels are critical for *Aspergillus fumigatus* virulence

Given the trehalose, cell wall, and biofilm phenotypes associated with alterations in SsdA levels, we hypothesized that SsdA plays an important role in *A. fumigatus* fungal-host interactions. To understand the importance of SsdA in the *A. fumigatus*-host interaction, we first utilized the triamcinolone (steroid) murine model of IPA (58). Strikingly, we observed that overexpression of SsdA significantly decreased *A. fumigatus* virulence compared to the wild type ($P = 0.0033$, OE:*ssdA* to the wild type) (**Fig. 6A**). This reduction in virulence was associated with a large reduction in immune cell infiltrate in the bronchoalveolar lavage fluid (BALs) ($P=0.0159$, OE:*ssdA* to the wild type, Mann-Whitney *t*-test) (**Fig. 6B**). Perhaps correspondingly, we observed a significant reduction in fungal growth within the OE:*ssdA* inoculated lungs compared to other strains (**Fig. 6C**).

In contrast, complete loss of SsdA did not alter median murine survival time between the wild type and Δ*ssdA* (median survival = 3 days). However, despite the *in vitro* growth defect of Δ*ssdA*, fungal burden observed by histopathology revealed modest increases in Δ*ssdA* fungal burden at day three post inoculation compared to wild-type (**Fig. 6C**). Surprisingly, despite equivalent or increased fungal burden compared to the wild type, a significant reduction in immune cell infiltrate in the bronchoalveolar lavage fluid (BALs) is apparent in animals inoculated with Δ*ssdA (*P=0.0159, Δ*ssdA* to the wild type, Mann-Whitney *t*-test) (**Fig. 6C**). These results support the hypothesis that changes in *ssdA* levels impact the fitness of *A. fumigatus in vivo* and alter host immune responses.

Given the striking Δ*ssdA in vitro* growth defect observed but full virulence (as measured by murine mortality) in the steroid IPA model, we hypothesized that SsdA would be essential for virulence in a leukopenic IPA model with significant immune cell depletion (41). However, surprisingly, and similar to the corticosteroid model, Δ*ssdA* also had persistent if not slightly increased virulence in the leukopenic model (*P = 0.005)* (**Fig. 6D**). Also similar to the steroid model, OE:*ssdA* had significant virulence attenuation compared to the wild type (*P* = 0.0049) (**Fig. 6D**). Median survival of the wild type, Δ*ssdA*, and OE:*ssdA*-inoculated mice was 3.5, 2, and 9.5 days, respectively. Histopathology from this leukopenic model revealed less fungal growth from lungs of OE:*ssdA*-inoculated mice while Δ*ssdA*-inoculated mice, in contrast to the *in vitro* growth phenotype, had substantial invasive hyphal growth compared to the wild type (**Fig. 6F**). In contrast to the steroid model, inflammatory cell infiltrations were the same between *ssdA* mutants and the wild type in this leukopenic model possibly reflecting the significant chemical mediated immune suppression (**Fig. 6E**). These results suggest that increased *ssdA* mRNA levels attenuate *A. fumigatus* virulence likely through fungal fitness defects while loss of SsdA alters the host immune response and modestly increases fungal virulence *in vivo*.

Discussion

The cell wall of *Aspergillus fumigatus* consists of polysaccharides including chitin, β-glucan, galactosaminogalactan, and others that are critical for fungal fitness in diverse environments including those associated with pathogenesis (29-38). Cell wall homeostasis and integrity are critical for the synthesis of each cell wall component in the face of stress and affect fungal pathogenesis on multiple levels (59). Another carbohydrate produced by fungi, trehalose, is also critical for fungal fitness during environmental stress including pathogenesis (42, 60). Previous research in multiple fungi has revealed an unexpected and ill-defined link between cell wall homeostasis and the biosynthesis of the disaccharide sugar trehalose (39-41). In *A. fumigatus,* a physical interaction between the TslA trehalose biosynthesis regulatory sub-unit and CsmA, a class V chitin synthase, suggested that trehalose biosynthesis proteins have direct roles in coordinating trehalose and fungal cell wall biosynthesis (41). Coordination between these 2 biological processes is logical given that both biosynthetic pathways utilize common carbohydrate metabolic intermediates. Intriguingly in our previous study, TslA was observed to physically interact with a protein (SsdA) that here we define as a homolog of the *S. cerevisiae* translational repressor protein Ssd1p. Alterations in the levels of SsdA in *A. fumigatus* impact both trehalose levels and cell wall integrity. Thus, these data further support the hypothesis that trehalose and cell wall biosynthesis are coordinated and implicate a new potential regulatory protein SsdA in these processes in *A. fumigatus*.

How physical interactions between TslA, SsdA, and CsmA in *A. fumigatus* mediate chitin and trehalose biosynthesis remains unclear. In *S. cerevisiae,* Ssd1p is a unique RNA-binding protein associated with multiple biological processes (43, 44) including stress tolerance, membrane trafficking, cell cycle, posttranslational modifications, mini-

297 chromosome stability, and cell wall integrity (45-47, 61). With regard to a regulatory role in
298 cell wall biosynthesis in yeast, Hogan, *et al.* (2008) showed that mRNA transcripts associated
299 with Ssd1 encoded proteins related to cell-wall biosynthesis, cell-wall remodeling and
300 regulation, cell cycle, and protein trafficking (44). Loss of *Sc*Ssd1p from both human and
301 plant yeast isolates impacted cell wall composition by increasing both chitin and mannan
302 content while decreasing β-1,3-glucan (50). Intriguingly, these results in yeast are opposite to
303 those observed here in *A. fumigatus* where SsdA loss appears to decrease chitin content while
304 overexpression of SsdA increased chitin. However, additional cell wall composition
305 biochemical assays are needed to define the impact of SsdA on cell wall composition.
306 Ssd1 homologs are also associated with cell wall integrity in the human pathogenic
307 yeast *Cryptococcus neoformans* though a *ssd1* loss of function strain displayed only modest
308 susceptibility to cell wall perturbing agents in this pathogenic yeast (62). However, a Ssd1
309 homolog in the human pathogenic yeast *Candida albicans* is associated with cell wall
310 integrity and virulence. Increased expression of *CaSSD1* is associated with antimicrobial
311 peptide resistance, while *ssd1* deletion mutants exhibit decreased virulence in an invasive
312 candidiasis murine model (51). Intriguingly, *Ca*Ssd1p physically interacts with *Ca*Cbk1p, an
313 NDR kinase (Nuclear Dbf2-related), which is important for hyphal morphogenesis, the RAM
314 pathway (Regulation of Ace2 and Morphogenesis), polarized growth, cell proliferation,
315 apoptosis, and cell wall biosynthesis (63, 64). *Ca*Ssd1p has nine *Ca*Cbk1p phosphorylation
316 consensus motifs. *Ca*Cbk1p is essential for Ssd1p localization to polarized growth areas (63).
317 Moreover, in the filamentous fungus *Neurospora crassa,* a *gul-1* (Ssd1 homolog) mutant is
318 able to partially suppress the severe fitness defect of a *cot-1* (Cbk1 homolog) temperature
319 sensitive mutant and this is associated with a reduction in transcript levels of cell wall
320 homeostasis genes including chitin synthases and the beta 1,3 glucan synthase *fks1* (54, 65).
321

322 The putative *A. fumigatus* Cbk1 homolog (AFUB_068890) is uncharacterized, but the
323 corresponding homolog in *A. nidulans*, CotA, is a conditionally essential gene and it is
324 unclear if it plays a direct role in cell wall or trehalose biosynthesis (66-68). However, loss of
325 *A. nidulans cotA* phenotypes can be suppressed by osmotic stabilization perhaps suggesting
326 an important role for this kinase in cell wall biosynthesis in *Aspergillus* spp (68). Future
327 experiments with *cotA* loss and/or gain of function mutants in *A. fumigatus* may reveal if this
328 important kinase plays a role in chitin synthase regulation and whether this role is mediated
329 by TslA and/or SsdA. Additional domain specific mutations in TslA/SsdA and/or genetic
330 screens may also help reveal the mechanistic relationship(s) behind the TslA-SsdA protein-
331 protein interaction and chitin biosynthesis.
332 Importantly for human fungal pathogenesis, our results suggest *A. fumigatus* SsdA
333 plays a role virulence. Clinical and plant yeast isolates with null mutations in *Scssd1*
334 have increased virulence in a DBA/2 murine infection model (50). *Scssd1* null mutants
335 induced more pro-inflammatory cytokine production perhaps consistent with alterations in
336 cell wall composition in Ssd1 mutants (50). In the fungal plant pathogens *Colletotrichum*
337 *lagenarium* and *Magnaporthe oryzae*, *SSD1* is also important for pathogenesis (52). It was
338 hypothesized that *SSD1* supported plant infection by evading induction of the plant immune
339 response (52). Interestingly, in *A. fumigatus* the loss of SsdA resulted in virulence similar to
340 wild-type strain as measured by murine mortality in both the corticosteroid and leukopenic
341 murine IPA models despite the *in vitro* colony and planktonic growth defects associated with
342 *ssdA* loss. In fact, in both murine models loss of *ssdA* appeared to promote *in vivo* fungal
343 growth but intriguingly reduced the host immune response. In contrast, overexpression of
344 SsdA severely attenuated virulence and we observed significantly less fungal growth in the
345 OE:*ssdA*-inoculated lungs suggesting that loss of virulence in this strain may be due to poor
346 *in vivo* fitness. The extreme adherence defect of OE:*ssdA* may contribute to this loss of *in*

vivo fungal burden and virulence, but we cannot rule out other mechanisms impacted by increased *SsdA* levels. For example, the significant delay in conidia *in vitro* germination observed in the OE:*ssdA* strain may also manifest *in vivo* and give the host immune system additional time to clear the fungus. Perhaps consistent with altered cell wall composition and PAMP exposure, both *ssdA* and OE:*ssdA*-inoculated BALF had decreased inflammatory cell infiltration, particularly neutrophils, and how these alterations in the host inflammatory response mediated infection outcomes in the presence and absence of SsdA require further investigation.

In conclusion, we identified a critical role for *A. fumigatus* SsdA in cell wall homeostasis, trehalose production, and virulence. SsdA is involved in regulation of chitin biosynthesis and/or homeostasis in this fungus, however, the mechanisms of this regulation are still unclear and further investigation is needed to fully understand the roles and mechanisms of SsdA in *A. fumigatus* cell wall integrity and fungal-host interactions. While there is a clear conservation of a role for SsdA homologs in cell wall homeostasis in many fungi, these data in *A. fumigatus* provide another example of altered wiring/functions of key master regulatory genes in pathogenic fungi compared to model organisms. It will also be interesting and important to explore the regulation and function of these pathways within fungal species to identify broadly conserved mechanisms for potential therapeutic development.

Materials and methods

Fungal strains, media, and growth conditions

Aspergillus fumigatus strain CEA17 strain (a uracil auxotroph strain lacking *pyrG* gene) was used to generate the *ssdA* null mutant (69). A *ku80* strain (a uracil auxotroph strain lacking *pyrG* and *akuB* genes) was used to generate S-tagged and Flag-tagged strains for pulldown

assays and co-immunoprecipitation experiments (69, 70). Glucose minimal media (GMM) containing 1% glucose were used to grow the mutants along with a wild type, CEA10 (CBS144.89) at 37°C with 5% CO_2 if not stated otherwise (71). The conidia from each strain were collected in 0.01% Tween-80 after 72-hour incubation at 37°C with 5% CO_2. Fresh conidia were used in all experiments.

Strain construction and fungal transformation

Gene replacements and reconstituted strains were generated as previously described (40, 58). PCR and Southern blot were used to confirm the mutant strains (40). Real-time reverse transcriptase PCR was used to confirm expression of the re-introduced gene and overexpressed strain (72). To generate the single-null mutant, *A. parasiticus pyrG* from pJW24 was used as a selectable marker (73). To generate reconstituted strains of single null mutants, we utilized a *ptrA* marker, which is a pyrithiamine resistance gene from *A. oryzae* (74). To generate GFP-tagged strains, we utilized a *hygB* marker, which is a hygromycin B phosphotransferase gene as a hygromycin resistant marker (75). For S-tagged strains, an S-tag coding sequence along with *AfpyrG* was introduced to the C-terminus of proteins of interest, i.e. TslA (76, 77). For co-immunoprecipitation experiments, we introduced GFP-tag with a *hygB* marker into C-terminus of SsdA in the background of C-terminal Flag-tagged CsmA with *pyrG* as a marker (78). In localization experiments, we generated C-terminal GFP-tagged CsmA in both the wild type (CEA17) and the Δ*ssdA* background by using *pyrG* and *ptrA* as a selectable marker, respectively. After the constructs were generated, polyethylene glycol-mediated transformation of fungal protoplasts was performed as previously described (79). For the *ptrA*-marker transformation, we added pyrithiamine hydrobromide (Sigma P0256) into 1.2 M sorbitol (SMM) media at 0.1 mg/L (74). For the *hygB*-marker transformation, we recovered the strains containing the *hygB* marker by adding

hygromycin B (Calbichem 400052) into the 0.7% top SMM agar at 150 μg/mL the day after transformation (75).

Germination assays and Biomass assays

10^8 conidia in 100mL LGMM of each strain were cultured at 37°C in three biological replicates. 500 μL of each culture was taken to count for germling percentage at indicated time points. For biomass assays, 10^8 conidia in 100mL LGMM of each strain were cultured for 24 hours at 37°C in three biological replicates. The biomass was collected, lyophilized and dry weight was recorded.

Cell wall perturbing agents and antifungal agents

Several cell-wall perturbing agents were utilized for cell wall integrity tests: Congo red (CR, Sigma C6277), Calcofluor white (CFW, Fluorescent brightener 28, Sigma F3543), and Caspofungin (CPG, Cancidas, MERCK&CO., INC.). CR, CFW, or CPG were added into GMM plates at final concentrations of 1 mg/mL, 50 μg/mL, and 1 μg/mL, respectively. Dropout assays were performed by plating serial conidial dilutions from $1x10^5$ to $1x10^2$ conidia in a 5-μL drop of each strain. The plates were cultured at 37°C with 5% CO_2 and the images were taken at 48 hours. This experiment was performed in three biological replicates (40).

Cell-wall PAMP exposure

Calcofluor white (CFW, 25μg/mL), fluorescein-labeled wheat germ agglutinin (WGA, 5 μg/mL) (Vector labs: FL-1021), and soluble dectin-1 staining were performed as previously described (80, 81). Briefly, each fungal strain was cultured until it reached the germination stage on liquid glucose minimal media. The hyphae were UV irradiated at 6,000 mJ/cm^2. The

micrographs were taken by the Z-stack of the fluorescent microscope, Zeiss HAL 100 (Carl Zeiss Microscopy, LLC, Thornwood, NY, USA) equipped with a Zeiss Axiocam MRm camera. The intensity was analyzed using ImageJ and the corrected total cell fluorescence (CTCF) was calculated (80, 82). Data are represented as mean +/- SE of 15 images from three biological replicates.

Adherence Assay and Biofilm Microscopy

For the crystal violet adherence assay, 100µL of 10^5 spores per mL in GMM were inoculated into U-bottomed 96-well plates and grown for 24 hours at 37ºC. Plates were washed with H_2O twice, stained with 0.1% (w/v) crystal violet in water for 10 minutes, washed twice more with H_2O to remove excess stain, and destained with 100% ethanol for 10 minutes. An aliquot of the de-stained supernatants were transferred to a flat-bottomed 96-well plate and Abs_{600} was measured using a plate reader. Results were analyzed using a One-Way ANOVA with a Tukey post-test. For microscopy, 10^5 spores per mL in GMM were grown for 24 hours at 37ºC on Mattek dishes (Mattek: P35G-1.5-10-C). Biofilms were stained with 20µg/mL FITC-SBA (Vector Labs: FL-1011) and fixed with 1% paraformaldehyde. Stained biofilms were imaged using a 20X-multi-immersion objective on an Andor W1 Spinning Disk Confocal with a Nikon Eclipse Ti inverted microscope stand with Perfect Focus and equipped with two Andor Zyla cameras and ASI MS-2000 stage. Z-stacks of the first 300-320µm were taken for each sample. Microscopy was performed on three biological replicates per strain.

RNA Extraction and qRT-PCR

RNA was extracted from 24-hour biofilms grown at 37ºC in GMM. Briefly, fungal tissue was flash frozen and bead beat with 2.3mm zirconia/silica beads in 200 µl of TriSure (Bioline:

447 BIO-38032). Homogenized mycelia were brought to a final volume of 1mL and RNA was
448 processed according to manufacturer's instructions. For qRT-PCR, 5ug of RNA was DNAse
449 treated with Ambion Turbo DNAse (Life Technologies) according to the manufacturer's
450 instruction. For qRT-PCR DNase treated-RNA was processed as previously described (83).
451 mRNA levels were normalized to *tef1* for all qRT-PCR analyses. Statistical analysis was
452 performed with One-Way ANOVA with Tukey post-test. Error bars indicate standard
453 deviation of the mean (SD).
454
455 **Chitin synthase activity assay**
456 10^8 conidia of each fungal strain were grown at 37°C for 24 hours in 10mL of liquid GMM at
457 250 rpm. The mycelia were collected to prepare of membrane fractions by a centrifugation at
458 100,000g for 40 min at 4°C as described before. After that, the nonradioactive chitin synthase
459 activity assay was performed in a 96-well plate as previously described (56, 57).
460
461 **Trehalose measurement**
462 Trehalose content in conidia and mycelia was as previously described (40). Briefly, *A.*
463 *fumigatus* strains were grown on GMM plates at 37°C for 3 days. A total of 2 x 10^8 conidia
464 were used for the conidial stage of the trehalose assay, and 1 x 10^8 conidia in 10mL LGMM
465 were cultured overnight for the mycelial stage as described by d'Enfert C and Fontaine
466 (1997) (53). Cell-free extracts were then tested for trehalose levels according to the Glucose
467 Assay Kit protocols (Sigma AGO20). Results from biological triplicate experiments were
468 averaged, standard deviation calculated, and statistical significance determined ($P < 0.05$)
469 with a two-tailed Student's *t*-test.
470
471 **Murine models of invasive pulmonary aspergillosis**

CD1 female mice, 6–8 weeks old, were used in the triamcinolone (steroid) or the chemotherapeutic murine model experiments as previously described (40, 41, 58). Mice were obtained from Charles River Laboratories (Raleigh, NC). For survival studies and histopathology, 10 mice per *A. fumigatus* strain (CEA10, Δ*ssdA*, *ΔssdA+ssdA-GFP*, and OE:*ssdA*) were inoculated intranasally with $2x10^6$ conidia in 40 µL of phosphate-buffered saline (PBS) for the triamcinolone model and $1x10^6$ conidia for the chemotherapeutic model, and monitored three times a day. Mice were observed for 14 days after the *A. fumigatus* challenge. Any animals showing distress were immediately humanely sacrificed and recorded as deaths within 24 hrs. No mock inoculated animals perished. Statistical comparison of the associated Kaplan-Meier curves was conducted with log rank tests (84). Lungs from all mice sacrificed at different time points during the experiment were removed for differential cell count and histopathology.

Histopathology

Three mice in each group (CEA10, Δ*ssdA*, *ΔssdA+ssdA-GFP*, and OE:*ssdA*) were humanely euthanized at day 3 post-inoculation. Lungs were harvested from each group and fixed in 10% formalin before embedding in paraffin. 5µm-thick sections were taken and stained with either H&E (Hematoxylin and Eosin) or GMS (Gomori-Methenamine Silver stain) as previously described (85). The microscopic examination was performed on a Zeiss Axioplan II microscope and engaged imaging system. Images were captured at 50x magnification as indicated in each image.

Collection and analysis of bronchoalveolar lavage fluid (BALF)

At the indicated time after *A. fumigatus* instillation, mice were euthanized using CO_2. Bronchoalveolar lavage fluid (BALF) was collected by washing the lungs with 2 mL of PBS containing 0.05M EDTA. BALF was then centrifuged and the supernatant collected and

497 stored at -20°C until analysis. BAL cells were resuspended in 200 µl of PBS and counted on a
498 hemocytometer to determine total cell counts. Cells were then spun onto glass slides using a
499 Thermo Scientific Cytospin4 cytocentrifuge and subsequently stained with a Diff-Quik
500 staining kit (Electron Microscopy Sciences) for differential cell counting (80).
501
502 **Ethics statement**
503 This study was carried out in strict accordance with the recommendations in the Guide for the
504 Care and Use of Laboratory Animals of the National Institutes of Health. The animal
505 experimental protocol was approved by the Institutional Animal Care and Use Committee
506 (IACUC) at Dartmouth College (protocol number cram.ra.1).
507
508

509 ## Acknowledgments

510 We thank the members of the microscope facilities in the Department of Biology at
511 Dartmouth College. A.T. thanks Dr. Dawoon Chung for initial training in *A. fumigatus*
512 molecular genetics techniques. A.T. and R.A.C. thank Dr. Jarrod Fortwendel for the chitin
513 synthase activity assay protocol and Thomas Hampton for suggestions on statistical analysis.
514 A.T. also thanks the Department of Microbiology, Faculty of Medicine, Chulalongkorn
515 University, Bangkok, Thailand for fellowship support.
516

517 ## Funding information

518 HHS | NIH | National Institute of Allergy and Infectious Diseases (NIAID)
519 R01AI081838 Robert A. Cramer; Burroughs Wellcome Fund (BWF) Robert A. Cramer;
520 National Institute of General Medicine Sciences (NIGMS)P30GM106394 Bruce Stanton;

JK is supported in part by NIH/NIAID T32AI007519. The funders had no role in study design, data collection and analysis, decision to publish, or preparation of the manuscript.

References

1. Brown GD, Denning DW, Gow NA, Levitz SM, Netea MG, White TC. 2012. Hidden killers: human fungal infections. Sci Transl Med 4:165rv13.
2. Zonios DI, Bennett JE. 2008. Update on azole antifungals. Semin Respir Crit Care Med 29:198-210.
3. Rex JH, Stevens DA. 2015. Drugs Active against Fungi, Pneumocystis, and Microsporidia, p 479-494e4. *In* Bennett JE, Dolin R, M.J. B (ed), Mandell, Douglas, and Bennett's Principles and Practice of Infectious Diseases, 8th ed. Saunders.
4. Mihaila RG. 2015. Voriconazole and the liver. World J Hepatol 7:1828-33.
5. Sawaya BP, Weihprecht H, Campbell WR, Lorenz JN, Webb RC, Briggs JP, Schnermann J. 1991. Direct vasoconstriction as a possible cause for amphotericin B-induced nephrotoxicity in rats. J Clin Invest 87:2097-107.
6. Vermeulen E, Maertens J, De Bel A, Nulens E, Boelens J, Surmont I, Mertens A, Boel A, Lagrou K. 2015. Nationwide Surveillance of Azole Resistance in Aspergillus Diseases. Antimicrob Agents Chemother 59:4569-76.
7. Fuhren J, Voskuil WS, Boel CH, Haas PJ, Hagen F, Meis JF, Kusters JG. 2015. High prevalence of azole resistance in Aspergillus fumigatus isolates from high-risk patients. J Antimicrob Chemother 70:2894-8.
8. de Fontbrune FS, Denis B, Meunier M, Garcia-Hermoso D, Bretagne S, Alanio A. 2014. Iterative breakthrough invasive aspergillosis due to TR(34) /L98H azole-resistant Aspergillus fumigatus and Emericella sublata in a single hematopoietic stem cell transplant patient. Transpl Infect Dis 16:687-91.
9. Burgel PR, Baixench MT, Amsellem M, Audureau E, Chapron J, Kanaan R, Honore I, Dupouy-Camet J, Dusser D, Klaassen CH, Meis JF, Hubert D, Paugam A. 2012. High prevalence of azole-resistant Aspergillus fumigatus in adults with cystic fibrosis exposed to itraconazole. Antimicrob Agents Chemother 56:869-74.
10. Jensen RH, Hagen F, Astvad KM, Tyron A, Meis JF, Arendrup MC. 2016. Azole-resistant Aspergillus fumigatus in Denmark: a laboratory-based study on resistance mechanisms and genotypes. Clin Microbiol Infect 22:570 e1-9.
11. Brillowska-Dabrowska A, Mroczynska M, Nawrot U, Wlodarczyk K, Kurzyk E. 2015. Examination of cyp51A and cyp51B expression level of the first Polish azole resistant clinical Aspergillus fumigatus isolate. Acta Biochim Pol 62:837-9.
12. Lazzarini C, Esposto MC, Prigitano A, Cogliati M, De Lorenzis G, Tortorano AM. 2015. Azole Resistance in Aspergillus fumigatus Clinical Isolates from an Italian Culture Collection. Antimicrob Agents Chemother 60:682-5.
13. Steinmann J, Hamprecht A, Vehreschild MJ, Cornely OA, Buchheidt D, Spiess B, Koldehoff M, Buer J, Meis JF, Rath PM. 2015. Emergence of azole-resistant invasive aspergillosis in HSCT recipients in Germany. J Antimicrob Chemother 70:1522-6.
14. Howard SJ, Cerar D, Anderson MJ, Albarrag A, Fisher MC, Pasqualotto AC, Laverdiere M, Arendrup MC, Perlin DS, Denning DW. 2009. Frequency and evolution of Azole resistance in Aspergillus fumigatus associated with treatment failure. Emerg Infect Dis 15:1068-76.
15. Chowdhary A, Kathuria S, Randhawa HS, Gaur SN, Klaassen CH, Meis JF. 2012. Isolation of multiple-triazole-resistant Aspergillus fumigatus strains carrying the TR/L98H mutations in the cyp51A gene in India. J Antimicrob Chemother 67:362-6.
16. Chowdhary A, Sharma C, van den Boom M, Yntema JB, Hagen F, Verweij PE, Meis JF. 2014. Multi-azole-resistant Aspergillus fumigatus in the environment in Tanzania. J Antimicrob Chemother 69:2979-83.

17. Badali H, Vaezi A, Haghani I, Yazdanparast SA, Hedayati MT, Mousavi B, Ansari S, Hagen F, Meis JF, Chowdhary A. 2013. Environmental study of azole-resistant Aspergillus fumigatus with TR34/L98H mutations in the cyp51A gene in Iran. Mycoses 56:659-63.
18. Ahmad S, Khan Z, Hagen F, Meis JF. 2014. Occurrence of triazole-resistant Aspergillus fumigatus with TR34/L98H mutations in outdoor and hospital environment in Kuwait. Environ Res 133:20-6.
19. Kidd SE, Goeman E, Meis JF, Slavin MA, Verweij PE. 2015. Multi-triazole-resistant Aspergillus fumigatus infections in Australia. Mycoses 58:350-5.
20. Ozmerdiven GE, Ak S, Ener B, Agca H, Cilo BD, Tunca B, Akalin H. 2015. First determination of azole resistance in Aspergillus fumigatus strains carrying the TR34/L98H mutations in Turkey. J Infect Chemother 21:581-6.
21. Wu CJ, Wang HC, Lee JC, Lo HJ, Dai CT, Chou PH, Ko WC, Chen YC. 2015. Azole-resistant Aspergillus fumigatus isolates carrying TR(3)(4)/L98H mutations in Taiwan. Mycoses 58:544-9.
22. Chen Y, Lu Z, Zhao J, Zou Z, Gong Y, Qu F, Bao Z, Qiu G, Song M, Zhang Q, Liu L, Hu M, Han X, Tian S, Zhao J, Chen F, Zhang C, Sun Y, Verweij PE, Huang L, Han L. 2016. Epidemiology and Molecular Characterizations of Azole Resistance in Clinical and Environmental Aspergillus fumigatus Isolates from China. Antimicrob Agents Chemother 60:5878-84.
23. Pelaez T, Monteiro MC, Garcia-Rubio R, Bouza E, Gomez-Lopez A, Mellado E. 2015. First detection of Aspergillus fumigatus azole-resistant strain due to Cyp51A TR46/Y121F/T289A in an azole-naive patient in Spain. New Microbes New Infect 6:33-4.
24. Lavergne RA, Morio F, Favennec L, Dominique S, Meis JF, Gargala G, Verweij PE, Le Pape P. 2015. First description of azole-resistant Aspergillus fumigatus due to TR46/Y121F/T289A mutation in France. Antimicrob Agents Chemother 59:4331-5.
25. Hagiwara D, Takahashi H, Fujimoto M, Sugahara M, Misawa Y, Gonoi T, Itoyama S, Watanabe A, Kamei K. 2016. Multi-azole resistant Aspergillus fumigatus harboring Cyp51A TR46/Y121F/T289A isolated in Japan. J Infect Chemother 22:577-9.
26. Tangwattanachuleeporn M, Minarin N, Saichan S, Sermsri P, Mitkornburee R, Gross U, Chindamporn A, Bader O. 2016. Prevalence of azole-resistant Aspergillus fumigatus in the environment of Thailand. Med Mycol doi:10.1093/mmy/myw090.
27. Wiederhold NP, Gil VG, Gutierrez F, Lindner JR, Albataineh MT, McCarthy DI, Sanders C, Fan H, Fothergill AW, Sutton DA. 2016. First Detection of TR34 L98H and TR46 Y121F T289A Cyp51 Mutations in Aspergillus fumigatus Isolates in the United States. J Clin Microbiol 54:168-71.
28. Le Pape P, Lavergne RA, Morio F, Alvarez-Moreno C. 2016. Multiple Fungicide-Driven Alterations in Azole-Resistant Aspergillus fumigatus, Colombia, 2015. Emerg Infect Dis 22:156-7.
29. Georgopapadakou NH, Tkacz JS. 1995. The fungal cell wall as a drug target. Trends Microbiol 3:98-104.
30. Bernard M, Latge JP. 2001. *Aspergillus fumigatus* cell wall: composition and biosynthesis. Med Mycol 39 Suppl 1:9-17.
31. Bruneau JM, Magnin T, Tagat E, Legrand R, Bernard M, Diaquin M, Fudali C, Latge JP. 2001. Proteome analysis of *Aspergillus fumigatus* identifies glycosylphosphatidylinositol-anchored proteins associated to the cell wall biosynthesis. Electrophoresis 22:2812-23.
32. Beauvais A, Latge JP. 2001. Membrane and cell wall targets in *Aspergillus fumigatus*. Drug Resist Updat 4:38-49.

641 33. Fontaine T, Simenel C, Dubreucq G, Adam O, Delepierre M, Lemoine J, Vorgias CE,
642 Diaquin M, Latge JP. 2000. Molecular organization of the alkali-insoluble fraction of
643 *Aspergillus fumigatus* cell wall. J Biol Chem 275:41528.
644 34. Fontaine T, Simenel C, Dubreucq G, Adam O, Delepierre M, Lemoine J, Vorgias CE,
645 Diaquin M, Latge JP. 2000. Molecular organization of the alkali-insoluble fraction of
646 *Aspergillus fumigatus* cell wall. J Biol Chem 275:27594-607.
647 35. Mouyna I, Hartland RP, Fontaine T, Diaquin M, Simenel C, Delepierre M, Henrissat
648 B, Latge JP. 1998. A 1,3-beta-glucanosyltransferase isolated from the cell wall of
649 *Aspergillus fumigatus* is a homologue of the yeast Bgl2p. Microbiology 144 (Pt
650 11):3171-80.
651 36. Fontaine T, Hartland RP, Diaquin M, Simenel C, Latge JP. 1997. Differential patterns
652 of activity displayed by two exo-beta-1,3-glucanases associated with the *Aspergillus*
653 *fumigatus* cell wall. J Bacteriol 179:3154-63.
654 37. Hartland RP, Fontaine T, Debeaupuis JP, Simenel C, Delepierre M, Latge JP. 1996. A
655 novel beta-(1-3)-glucanosyltransferase from the cell wall of *Aspergillus fumigatus*. J
656 Biol Chem 271:26843-9.
657 38. Latge JP, Debeaupuis JP, Sarfati J, Diaquin M, Paris S. 1993. Cell wall antigens in
658 *Aspergillus fumigatus*. Arch Med Res 24:269-74.
659 39. Al-Bader N, Vanier G, Liu H, Gravelat FN, Urb M, Hoareau CM, Campoli P, Chabot
660 J, Filler SG, Sheppard DC. 2010. Role of trehalose biosynthesis in Aspergillus
661 fumigatus development, stress response, and virulence. Infect Immun 78:3007-18.
662 40. Puttikamonkul S, Willger SD, Grahl N, Perfect JR, Movahed N, Bothner B, Park S,
663 Paderu P, Perlin DS, Cramer RA, Jr. 2010. Trehalose 6-phosphate phosphatase is
664 required for cell wall integrity and fungal virulence but not trehalose biosynthesis in
665 the human fungal pathogen Aspergillus fumigatus. Mol Microbiol 77:891-911.
666 41. Thammahong A, Caffrey-Card AK, Dhingra S, Obar JJ, Cramer RA. 2017.
667 Aspergillus fumigatus Trehalose-Regulatory Subunit Homolog Moonlights To
668 Mediate Cell Wall Homeostasis through Modulation of Chitin Synthase Activity.
669 MBio 8.
670 42. Thammahong A, Puttikamonkul S, Perfect JR, Brennan RG, Cramer RA. 2017.
671 Central Role of the Trehalose Biosynthesis Pathway in the Pathogenesis of Human
672 Fungal Infections: Opportunities and Challenges for Therapeutic Development.
673 Microbiol Mol Biol Rev 81.
674 43. Uesono Y, Toh-e A, Kikuchi Y. 1997. Ssd1p of *Saccharomyces cerevisiae* associates
675 with RNA. J Biol Chem 272:16103-9.
676 44. Hogan DJ, Riordan DP, Gerber AP, Herschlag D, Brown PO. 2008. Diverse RNA-
677 binding proteins interact with functionally related sets of RNAs, suggesting an
678 extensive regulatory system. PLoS Biol 6:e255.
679 45. Uesono Y, Fujita A, Toh-e A, Kikuchi Y. 1994. The *MCS1/SSD1/SRK1/SSL1* gene is
680 involved in stable maintenance of the chromosome in yeast. Gene 143:135-8.
681 46. Kosodo Y, Imai K, Hirata A, Noda Y, Takatsuki A, Adachi H, Yoda K. 2001.
682 Multicopy suppressors of the *sly1* temperature-sensitive mutation in the ER-Golgi
683 vesicular transport in *Saccharomyces cerevisiae*. Yeast 18:1003-14.
684 47. Vannier D, Damay P, Shore D. 2001. A role for Sds3p, a component of the
685 Rpd3p/Sin3p deacetylase complex, in maintaining cellular integrity in *Saccharomyces*
686 *cerevisiae*. Mol Genet Genomics 265:560-8.
687 48. Kaeberlein M, Guarente L. 2002. *Saccharomyces cerevisiae MPT5* and *SSD1* function
688 in parallel pathways to promote cell wall integrity. Genetics 160:83-95.
689 49. Reinke A, Anderson S, McCaffery JM, Yates J, 3rd, Aronova S, Chu S, Fairclough S,
690 Iverson C, Wedaman KP, Powers T. 2004. TOR complex 1 includes a novel

component, Tco89p (YPL180w), and cooperates with Ssd1p to maintain cellular integrity in Saccharomyces cerevisiae. J Biol Chem 279:14752-62.
50. Wheeler RT, Kupiec M, Magnelli P, Abeijon C, Fink GR. 2003. A Saccharomyces cerevisiae mutant with increased virulence. Proc Natl Acad Sci U S A 100:2766-70.
51. Gank KD, Yeaman MR, Kojima S, Yount NY, Park H, Edwards JE, Jr., Filler SG, Fu Y. 2008. SSD1 is integral to host defense peptide resistance in Candida albicans. Eukaryot Cell 7:1318-27.
52. Tanaka S, Yamada K, Yabumoto K, Fujii S, Huser A, Tsuji G, Koga H, Dohi K, Mori M, Shiraishi T, O'Connell R, Kubo Y. 2007. Saccharomyces cerevisiae SSD1 orthologues are essential for host infection by the ascomycete plant pathogens Colletotrichum lagenarium and Magnaporthe grisea. Mol Microbiol 64:1332-49.
53. d'Enfert C, Fontaine T. 1997. Molecular characterization of the Aspergillus nidulans treA gene encoding an acid trehalase required for growth on trehalose. Mol Microbiol 24:203-16.
54. Herold I, Yarden O. 2017. Regulation of Neurospora crassa cell wall remodeling via the cot-1 pathway is mediated by gul-1. Curr Genet 63:145-159.
55. Gravelat FN, Beauvais A, Liu H, Lee MJ, Snarr BD, Chen D, Xu W, Kravtsov I, Hoareau CM, Vanier G, Urb M, Campoli P, Al Abdallah Q, Lehoux M, Chabot JC, Ouimet MC, Baptista SD, Fritz JH, Nierman WC, Latge JP, Mitchell AP, Filler SG, Fontaine T, Sheppard DC. 2013. Aspergillus galactosaminogalactan mediates adherence to host constituents and conceals hyphal beta-glucan from the immune system. PLoS Pathog 9:e1003575.
56. Fortwendel JR, Juvvadi PR, Perfect BZ, Rogg LE, Perfect JR, Steinbach WJ. 2010. Transcriptional regulation of chitin synthases by calcineurin controls paradoxical growth of Aspergillus fumigatus in response to caspofungin. Antimicrob Agents Chemother 54:1555-63.
57. Lucero HA, Kuranda MJ, Bulik DA. 2002. A nonradioactive, high throughput assay for chitin synthase activity. Anal Biochem 305:97-105.
58. Grahl N, Puttikamonkul S, Macdonald JM, Gamcsik MP, Ngo LY, Hohl TM, Cramer RA. 2011. In vivo hypoxia and a fungal alcohol dehydrogenase influence the pathogenesis of invasive pulmonary aspergillosis. PLoS Pathog 7:e1002145.
59. Valiante V, Macheleidt J, Foge M, Brakhage AA. 2015. The Aspergillus fumigatus cell wall integrity signaling pathway: drug target, compensatory pathways, and virulence. Front Microbiol 6:325.
60. Gancedo C, Flores CL. 2004. The importance of a functional trehalose biosynthetic pathway for the life of yeasts and fungi. FEMS Yeast Res 4:351-9.
61. Reinke CA, Kozik P, Glick BS. 2004. Golgi inheritance in small buds of Saccharomyces cerevisiae is linked to endoplasmic reticulum inheritance. Proc Natl Acad Sci U S A 101:18018-23.
62. Gerik KJ, Donlin MJ, Soto CE, Banks AM, Banks IR, Maligie MA, Selitrennikoff CP, Lodge JK. 2005. Cell wall integrity is dependent on the PKC1 signal transduction pathway in Cryptococcus neoformans. Mol Microbiol 58:393-408.
63. Lee HJ, Kim JM, Kang WK, Yang H, Kim JY. 2015. The NDR Kinase Cbk1 Downregulates the Transcriptional Repressor Nrg1 through the mRNA-Binding Protein Ssd1 in Candida albicans. Eukaryot Cell 14:671-83.
64. Saputo S, Norman KL, Murante T, Horton BN, Diaz Jde L, DiDone L, Colquhoun J, Schroeder JW, Simmons LA, Kumar A, Krysan DJ. 2016. Complex Haploinsufficiency-Based Genetic Analysis of the NDR/Lats Kinase Cbk1 Provides Insight into Its Multiple Functions in Candida albicans. Genetics 203:1217-33.

65. Terenzi HF, Reissig JL. 1967. Modifiers of the cot gene in Neurospora: the gulliver mutants. Genetics 56:321-9.
66. Johns SA, Leeder AC, Safaie M, Turner G. 2006. Depletion of Aspergillus nidulans cotA causes a severe polarity defect which is not suppressed by the nuclear migration mutation nudA2. Mol Genet Genomics 275:593-604.
67. Shi J, Chen W, Liu Q, Chen S, Hu H, Turner G, Lu L. 2008. Depletion of the MobB and CotA complex in Aspergillus nidulans causes defects in polarity maintenance that can be suppressed by the environment stress. Fungal Genet Biol 45:1570-81.
68. Gao L, Song Y, Cao J, Wang S, Wei H, Jiang H, Lu L. 2011. Osmotic stabilizer-coupled suppression of NDR defects is dependent on the calcium-calcineurin signaling cascade in Aspergillus nidulans. Cell Signal 23:1750-7.
69. d'Enfert C. 1996. Selection of multiple disruption events in Aspergillus fumigatus using the orotidine-5'-decarboxylase gene, pyrG, as a unique transformation marker. Curr Genet 30:76-82.
70. da Silva Ferreira ME, Kress MR, Savoldi M, Goldman MH, Hartl A, Heinekamp T, Brakhage AA, Goldman GH. 2006. The akuB(KU80) mutant deficient for nonhomologous end joining is a powerful tool for analyzing pathogenicity in Aspergillus fumigatus. Eukaryot Cell 5:207-11.
71. Shimizu K, Keller NP. 2001. Genetic involvement of a cAMP-dependent protein kinase in a G protein signaling pathway regulating morphological and chemical transitions in Aspergillus nidulans. Genetics 157:591-600.
72. Cramer RA, Jr., Gamcsik MP, Brooking RM, Najvar LK, Kirkpatrick WR, Patterson TF, Balibar CJ, Graybill JR, Perfect JR, Abraham SN, Steinbach WJ. 2006. Disruption of a nonribosomal peptide synthetase in Aspergillus fumigatus eliminates gliotoxin production. Eukaryot Cell 5:972-80.
73. Weidner G, d'Enfert C, Koch A, Mol PC, Brakhage AA. 1998. Development of a homologous transformation system for the human pathogenic fungus Aspergillus fumigatus based on the pyrG gene encoding orotidine 5'-monophosphate decarboxylase. Curr Genet 33:378-85.
74. Kubodera T, Yamashita N, Nishimura A. 2002. Transformation of Aspergillus sp. and Trichoderma reesei using the pyrithiamine resistance gene (ptrA) of Aspergillus oryzae. Biosci Biotechnol Biochem 66:404-6.
75. Cullen D, Leong SA, Wilson LJ, Henner DJ. 1987. Transformation of Aspergillus nidulans with the hygromycin-resistance gene, hph. Gene 57:21-6.
76. Liu HL, De Souza CP, Osmani AH, Osmani SA. 2009. The three fungal transmembrane nuclear pore complex proteins of Aspergillus nidulans are dispensable in the presence of an intact An-Nup84-120 complex. Mol Biol Cell 20:616-30.
77. Liu HL, Osmani AH, Ukil L, Son S, Markossian S, Shen KF, Govindaraghavan M, Varadaraj A, Hashmi SB, De Souza CP, Osmani SA. 2010. Single-step affinity purification for fungal proteomics. Eukaryot Cell 9:831-3.
78. Franceschetti M, Bueno E, Wilson RA, Tucker SL, Gomez-Mena C, Calder G, Sesma A. 2011. Fungal virulence and development is regulated by alternative pre-mRNA 3'end processing in Magnaporthe oryzae. PLoS Pathog 7:e1002441.
79. Bok JW, Keller NP. 2004. LaeA, a regulator of secondary metabolism in Aspergillus spp. Eukaryot Cell 3:527-35.
80. Shepardson KM, Ngo LY, Aimanianda V, Latge JP, Barker BM, Blosser SJ, Iwakura Y, Hohl TM, Cramer RA. 2013. Hypoxia enhances innate immune activation to Aspergillus fumigatus through cell wall modulation. Microbes Infect 15:259-69.
81. Wagener J, Malireddi RK, Lenardon MD, Koberle M, Vautier S, MacCallum DM, Biedermann T, Schaller M, Netea MG, Kanneganti TD, Brown GD, Brown AJ, Gow

NA. 2014. Fungal chitin dampens inflammation through IL-10 induction mediated by NOD2 and TLR9 activation. PLoS Pathog 10:e1004050.

82. Gavet O, Pines J. 2010. Progressive activation of CyclinB1-Cdk1 coordinates entry to mitosis. Dev Cell 18:533-43.

83. Beattie SR, Mark KMK, Thammahong A, Ries LNA, Dhingra S, Caffrey-Carr AK, Cheng C, Black CC, Bowyer P, Bromley MJ, Obar JJ, Goldman GH, Cramer RA. 2017. Filamentous fungal carbon catabolite repression supports metabolic plasticity and stress responses essential for disease progression. PLoS Pathog 13:e1006340.

84. Willger SD, Cornish EJ, Chung D, Fleming BA, Lehmann MM, Puttikamonkul S, Cramer RA. 2012. Dsc orthologs are required for hypoxia adaptation, triazole drug responses, and fungal virulence in Aspergillus fumigatus. Eukaryot Cell 11:1557-67.

85. Huppert M, Oliver DJ, Sun SH. 1978. Combined methenamine-silver nitrate and hematoxylin & eosin stain for fungi in tissues. J Clin Microbiol 8:598-603.

Figure legends

Fig 1. Alteration of *ssdA* expression affects trehalose production, hyphal growth, and conidia germination. (A) Trehalose assays were performed to measure trehalose at both the conidial and mycelial stages using a glucose oxidase assay. Data represented as mean +/- SE of three biological replicates. For the conidial stage, (***) indicates *P* value = 0.0004, unpaired two-tailed Student's *t*-test Δ*ssdA* to the wild type; (***) indicates *P* value < 0.0001, unpaired two-tailed Student's *t*-test compared OE:*ssdA* to the wild type. For the mycelial stage, (*) indicates *P* value = 0.0110, unpaired two-tailed Student's *t*-test Δ*ssdA* to the wild type; (**) indicates *P* value = 0.007, unpaired two-tailed Student's *t*-test OE:*ssdA* to the wild type. (B, C) Radial growth assays were performed with each strain using GMM at 37°C for 72 hours (B). Images are a representative image of three independent experiments with similar results. The measurement of the radial growth was performed at 72 hours (C). Data represented as mean +/- SE of three biological replicates. (***) indicates *P* value < 0.0001 (unpaired two-tailed Student's *t*-test compared to the wild-type CEA10). (D) Fungal biomass was measured using 10^8 spores in 100mL liquid GMM at 37°C for 24 hours. Data represented as mean +/- SE of three biological replicates. (*) indicates *P* value = 0.0133 and (**) indicates *P* value = 0.0023, unpaired two-tailed Student's *t*-test. (E) Germination assays were utilized using 10^8 spores in 10mL liquid GMM at 37°C. 500μL of each culture were taken to count for the percentage of germlings at each time point. Data represented as mean +/- SE of three biological replicates. (**) indicates *P* value <0.01, unpaired two-tailed Student's *t*-test, compared the *ssdA* null mutant to the wild type at 6-8 hours. (***) indicates *P*<0.0001, unpaired two-tailed Student's *t*-test, compared the overexpression strain to the wild type at 5-12 hours.

845

846 **Fig 2. SsdA is important for cell wall integrity.** Cell wall perturbing agents, i.e. 1 mg/mL
847 congo red, 50 μg/mL calcofluor white (CFW), and 2 μg/mL caspofungin, were utilized to
848 study cell wall integrity in the respective strains. Cultures were incubated at 37°C for 48
849 hours. Data are a representative image of three independent experiments all with similar
850 results.

851

852 **Fig 3. Alteration of *ssdA* expression affects exposure of cell wall PAMPs.** Calcofluor
853 white (CFW) staining (A), wheat germ agglutinin (WGA) (B), and soluble dectin-1 (sDectin-
854 1) staining (C) were utilized to observe chitin levels/exposure and the β-glucan exposure on
855 the cell wall of the respective strains. Each strain was cultured to the germling stage under
856 normoxic conditions at 37°C. The corrected total cell fluorescence (CTCF) was calculated.
857 For CFW staining, (*) indicates *P* value = 0.0322, unpaired two-tailed Student's *t*-test
858 compared Δ*ssdA* to the wild type; (***) indicates *P*<0.0001, unpaired two-tailed Student's *t*-
859 test compared OE:*ssdA* to the wild type. For WGA staining, (***) indicates *P* value =
860 0.0002, unpaired two-tailed Student's *t*-test compared Δ*ssdA* to the wild type; (***) indicates
861 *P* value = 0.0008, unpaired two-tailed Student's *t*-test compared OE:*ssdA* to the wild type.
862 For sDectin-1 staining, (*) indicates *P* value = 0.0389, unpaired two-tailed Student's *t*-test
863 compared Δ*ssdA* to the wild type; (***) indicates *P* value < 0.0001, unpaired two-tailed
864 Student's *t*-test compared OE:*ssdA* to the wild type. Data are represented as mean +/- SE of
865 15 images from three biological replicates. Scale bar 3 μm. AU, Arbitrary Unit.

866

867 **Fig 4. Expression of *ssdA* Impacts Adherence and Biofilm Formation (A).** Biofilms were
868 grown at 37ºC for 24 hours in wells of a 96 well plate and the crystal violet adherence assay
869 was performed. Bars represent 6 replicates per strain, and the experiment was repeated 3

times with the same results. (***) indicates *P* value < 0.0001 via One-Way ANOVA with a Tukey post-test. **(B).** Micrographs of 24-hour biofilms stained with FITC-conjugated soybean agglutinin. Images are looking down a Z-stack of the first 300-320μm of the biofilm. Images are representative of 3 biological replicate cultures. **(C).** RNA was obtained from 24-hour biofilm cultures and qRT-PCR was performed for *uge3* mRNA levels. Data were normalized to *tef1* transcript levels. (n.s.) indicates not significant by One-Way ANOVA with a Tukey post-test.

Fig 5. Chitin activity and CsmA localization (A). 10 μg of membrane proteins were used to perform a non-radioactive chitin synthase activity assay. Each strain was cultured at 30°C for 6 hours and switched to 37°C for 24 hours. (**) indicates *P* value = 0.0029, unpaired two-tailed Student's *t*-test compared Δ*csmA* to the wild type; (*) indicates *P* value = 0.0208, unpaired two-tailed Student's *t*-test compared Δ*ssdA* to the wild type; (***) indicates *P value* < 0.0001, unpaired two-tailed Student's *t*-test compared OE:*ssdA* to the wild type. Data represented as mean +/- SE of three biological replicates. (B) C-terminal GFP-tagged CsmA was generated in the wild type, Δ*ssdA*, *ΔssdA+ssdA,* and OE:*ssdA* backgrounds. Each strain was cultured at 37°C for 12 hours and live-cell imaging was performed under a Quorum Technologies WaveFX Spinning Disk Confocal Microscope (1000X). The images were analyzed using Imaris 8.1.4 software. Data are representative images of 15 images from three biological replicates. Scale bar 3 μm.

Figure 6. Overexpression of SsdA attenuates virulence in the triamcinolone murine model while both loss of SsdA (Δ*ssdA*) and overexpression of SsdA (OE:*ssdA*) alters immune cell infiltrates. (A) $2x10^6$ conidia of each strain were inoculated via the intranasal route in the corticosteroid IPA murine model. Ten CD1 mice were used in each group.

Survival analysis was performed for two weeks. (**) indicates *P* value = 0.0033, Log Rank test compared OE:*ssdA* to the wild type. (B) Δ*ssdA* and OE:*ssdA*-infected BALs had decreased total inflammatory cell infiltrations. Total cell count: (*) indicates *P* value = 0.0159, two-tailed Mann-Whitney *t*-test compared Δ*ssdA* to the wild type; (*) indicates *P* value = 0.0159, two-tailed Mann-Whitney *t*-test compared OE:*ssdA* to the wild type. (C) OE:*ssdA*-infected lungs show less fungal growth and less cell infiltration compared to the wild type. The fungal histology was performed on Day3 to observe fungal growth and inflammatory cell infiltrations. GMS, Gomori-methenamine silver staining; H&E: hematoxylin and eosin staining. Magnification 50x. (D) $1x10^6$ conidia of each strain were inoculated intranasally for the chemotherapeutic murine model and survival analyses were performed for two weeks using ten CD1 mice per group. For Δ*ssdA* mutant, (**) indicates *P* value = 0.005, Log Rank test. For OE:*ssdA*, (**) indicates *P value* = 0.0049, Log Rank test. (B) Δ*ssdA* and OE:*ssdA*-infected BALs had similar total inflammatory cell infiltrations to the wild type BALs.

(C) OE:*ssdA*-infected lungs showed less fungal growth compared to the wild type. Histology was performed on Day3 to observe fungal growth and inflammatory cell infiltration. GMS, Gomori-methenamine silver staining; H&E: hematoxylin and eosin staining. Magnification 50x and 100x.

A.

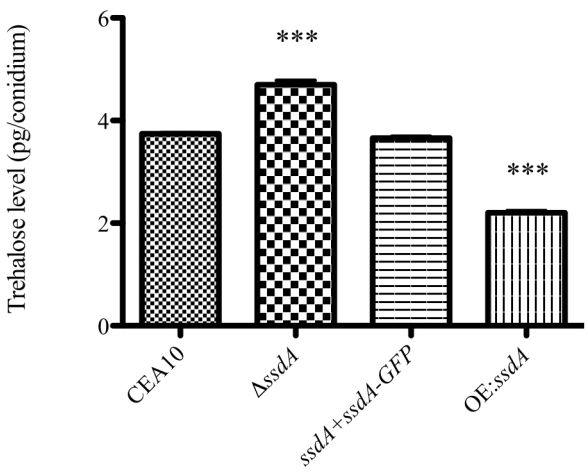
Conidial stage
Trehalose level (pg/conidium)
6
4
2
0
***
***
CEA10
ΔssdA
ssdA+ssdA-GFP
OE:ssdA

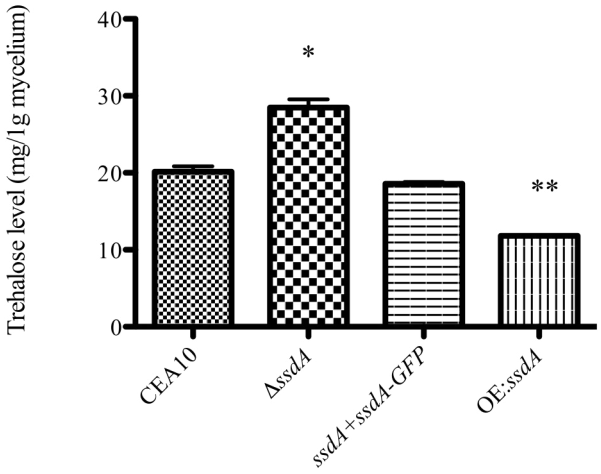
Mycelial stage
Trehalose level (mg/1g mycelium)
40
30
20
10
0
*
**
CEA10
ΔssdA
ssdA+ssdA-GFP
OE:ssdA

B.

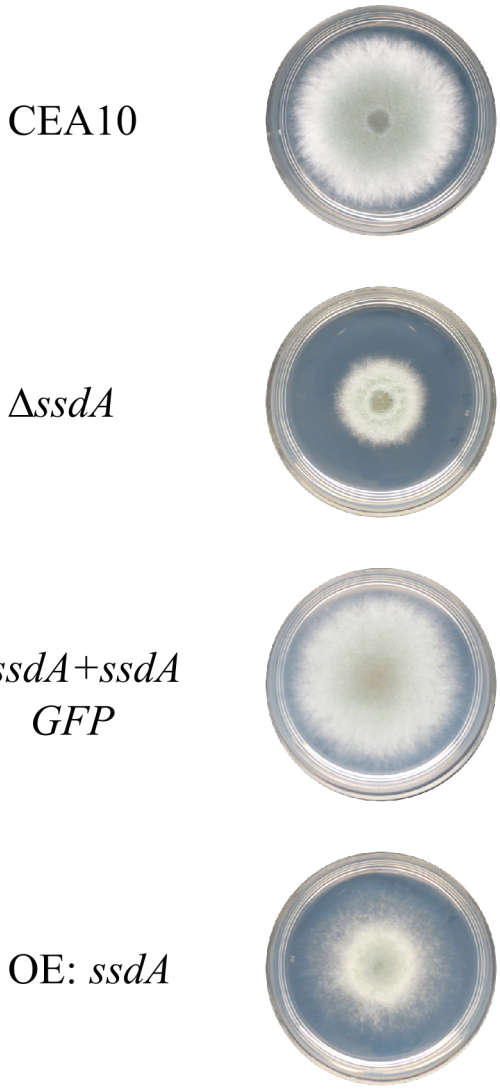
CEA10
ΔssdA
ΔssdA+ssdA GFP
OE: ssdA

C.

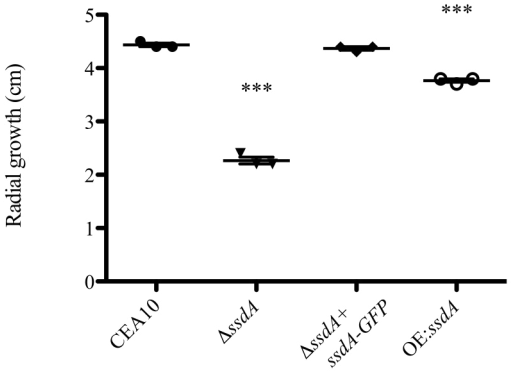
Radial growth (cm)
5
4
3
2
1
0
***
***
CEA10
ΔssdA
ΔssdA+ ssdA-GFP
OE:ssdA

D.

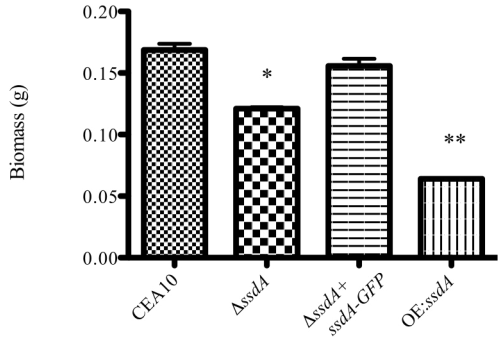
Biomass (g)
0.20
0.15
0.10
0.05
0.00
*
**
CEA10
ΔssdA
ΔssdA+ ssdA-GFP
OE:ssdA

E.

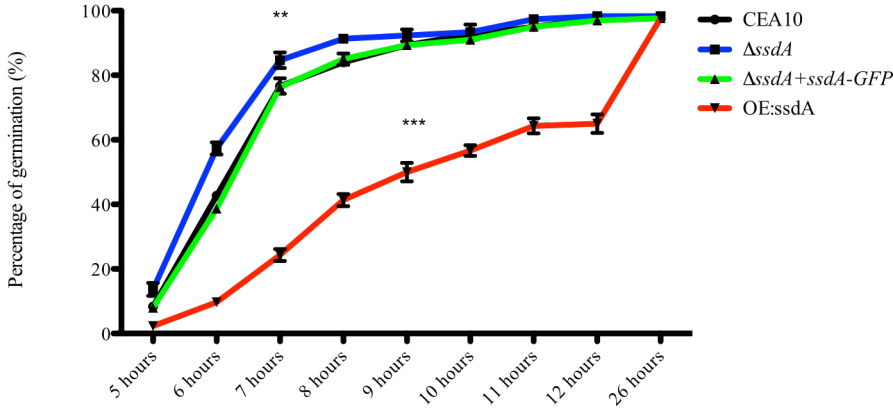
Percentage of germination (%)
100
80
60
40
20
0
**
***
5 hours
6 hours
7 hours
8 hours
9 hours
10 hours
11 hours
12 hours
26 hours
CEA10
ΔssdA
ΔssdA+ssdA-GFP
OE:ssdA

A.

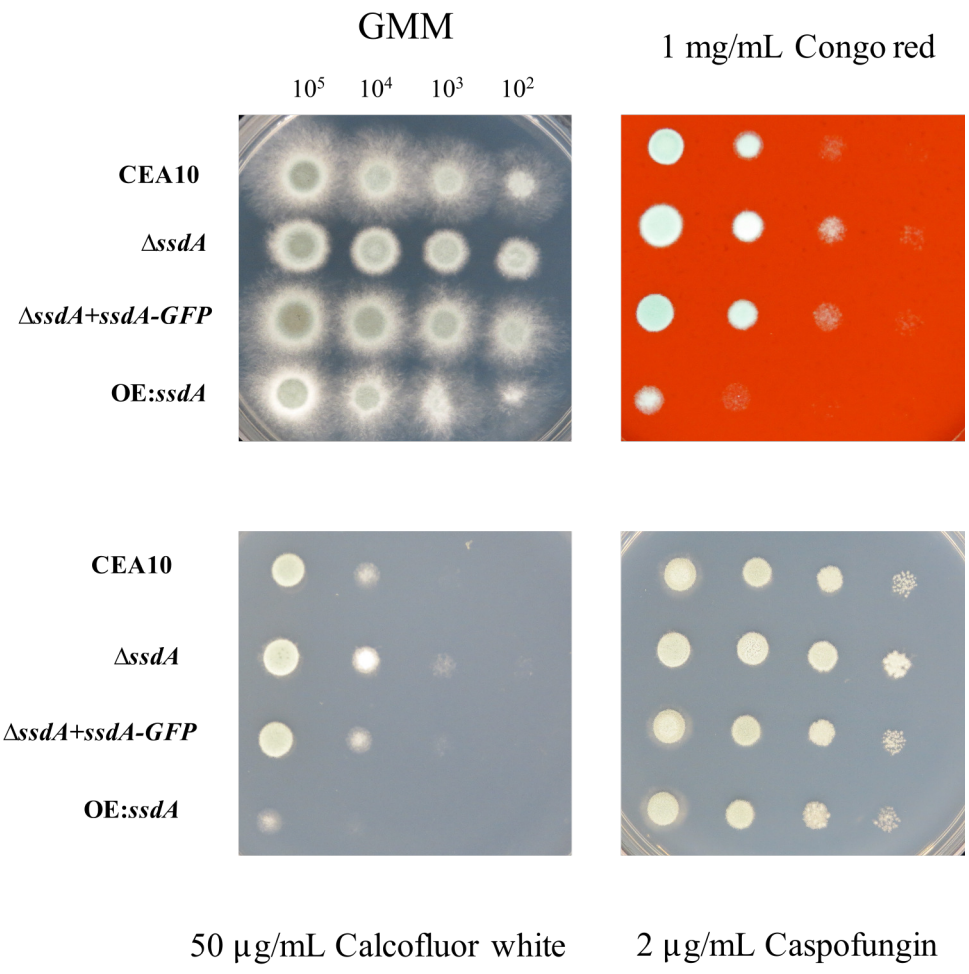
GMM
1 mg/mL Congo red
10^5 10^4 10^3 10^2
CEA10
ΔssdA
ΔssdA+ssdA-GFP
OE:ssdA
CEA10
ΔssdA
ΔssdA+ssdA-GFP
OE:ssdA
50 μg/mL Calcofluor white
2 μg/mL Caspofungin

A.

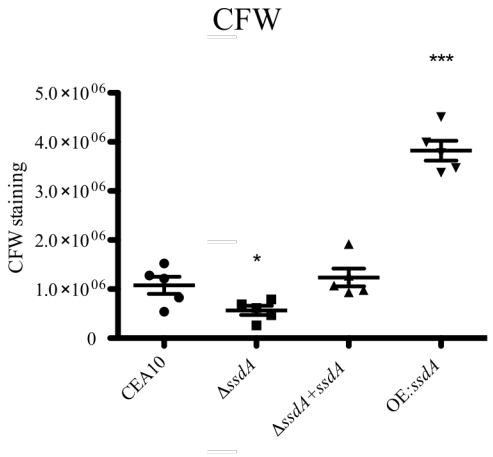
CFW
CFW staining
5.0×10^06
4.0×10^06
3.0×10^06
2.0×10^06
1.0×10^06
0
*
***
CEA10
ΔssdA
ΔssdA+ssdA
OE:ssdA

B.

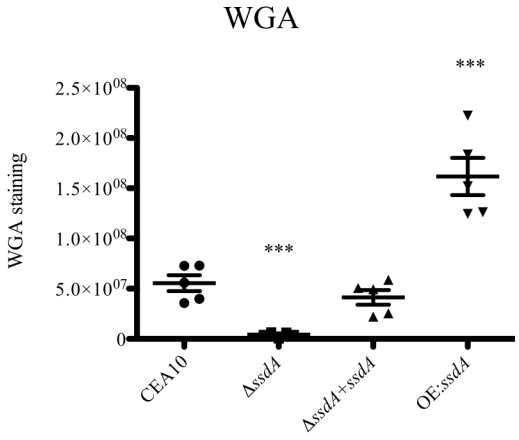
WGA
WGA staining
2.5×10^08
2.0×10^08
1.5×10^08
1.0×10^08
5.0×10^07
0
***
***
CEA10
ΔssdA
ΔssdA+ssdA
OE:ssdA

C.

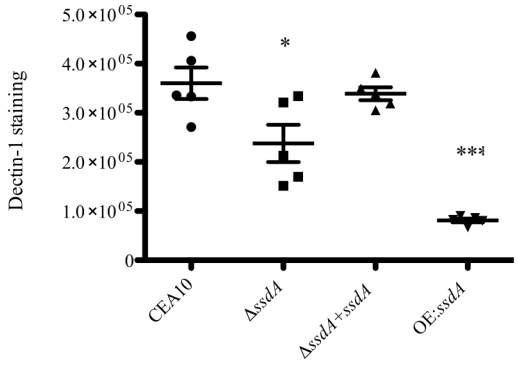
Dectin-1-Fc
Dectin-1 staining
5.0×10^05
4.0×10^05
3.0×10^05
2.0×10^05
1.0×10^05
0
*
***
CEA10
ΔssdA
ΔssdA+ssdA
OE:ssdA

A.

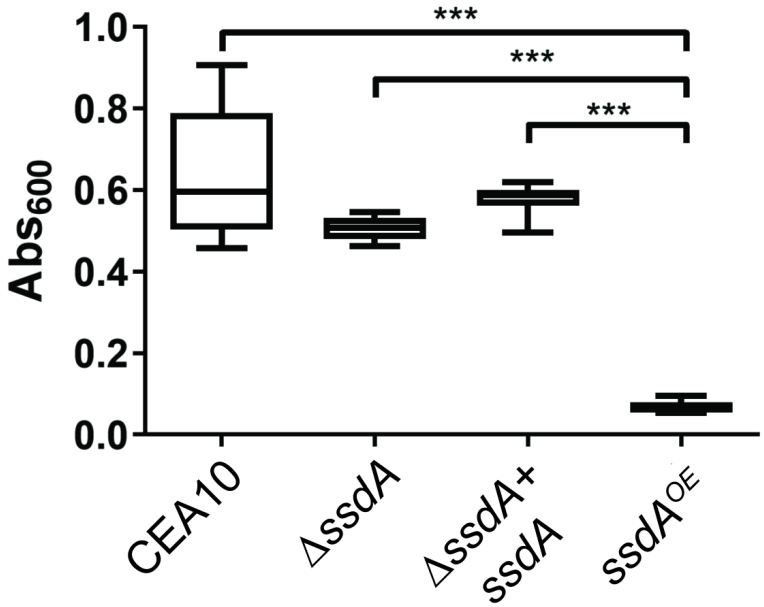
***
***
***
1.0
0.8
0.6
0.4
0.2
0.0
Abs600
CEA10
ΔssdA
ΔssdA+ ssdA
ssdAOE

B.

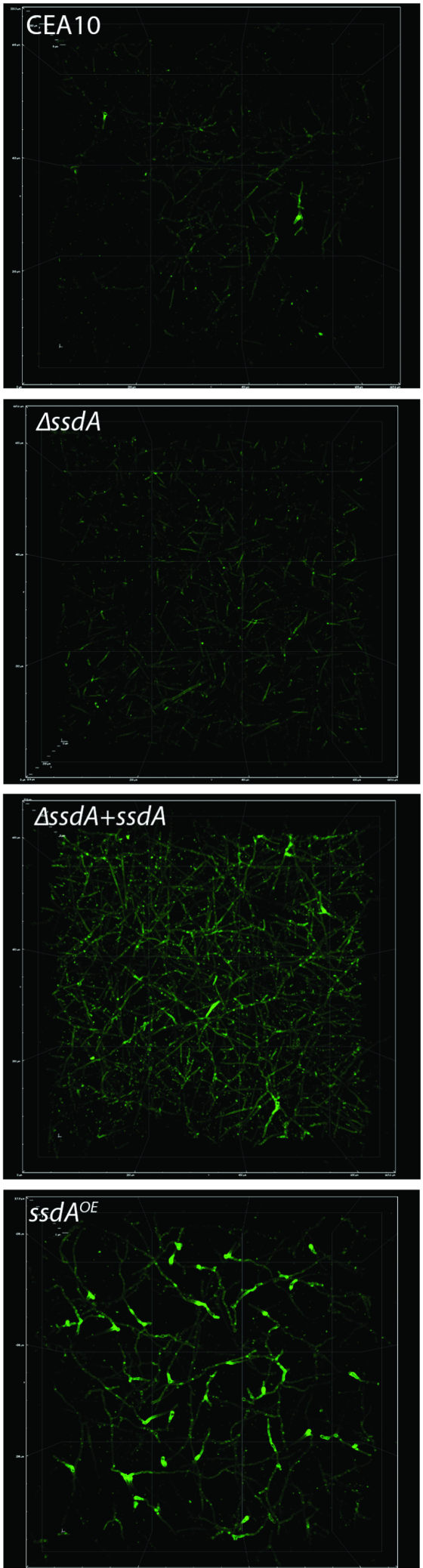
CEA10
ΔssdA
ΔssdA+ssdA
ssdAOE

C.

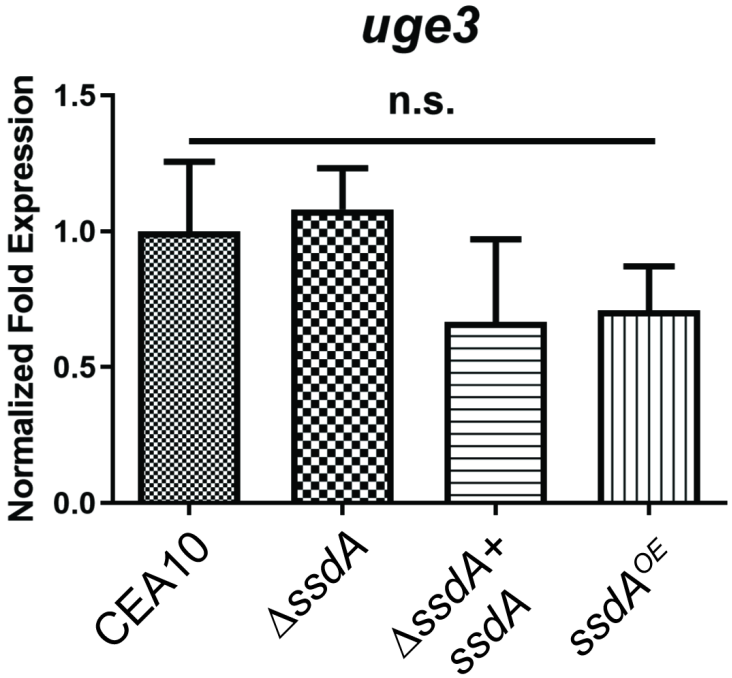
uge3
n.s.
1.5
1.0
0.5
0.0
Normalized Fold Expression
CEA10
ΔssdA
ΔssdA+ ssdA
ssdAOE

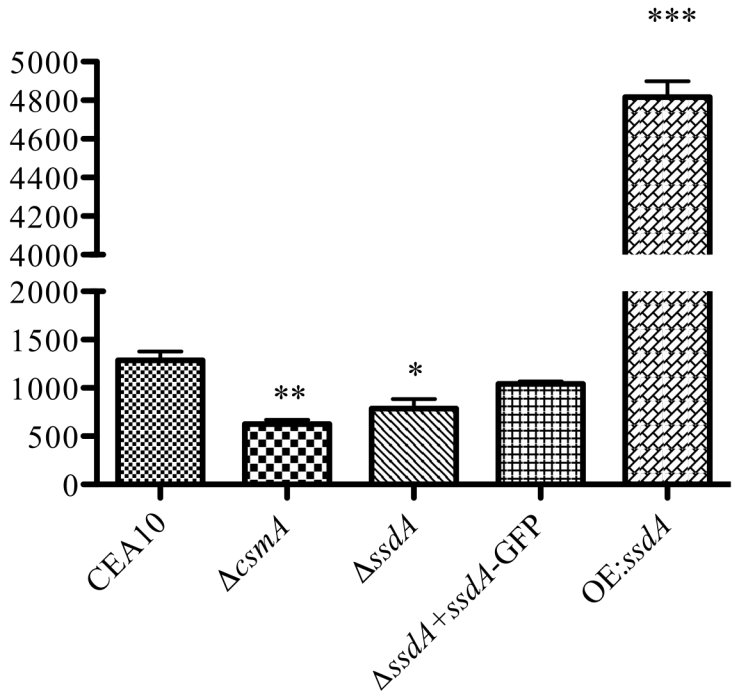
***
5000
4800
4600
4400
4200
4000
2000
1500
1000
500
0
**
*
CEA10
ΔcsmA
ΔssdA
ΔssdA+ssdA-GFP
OE:ssdA

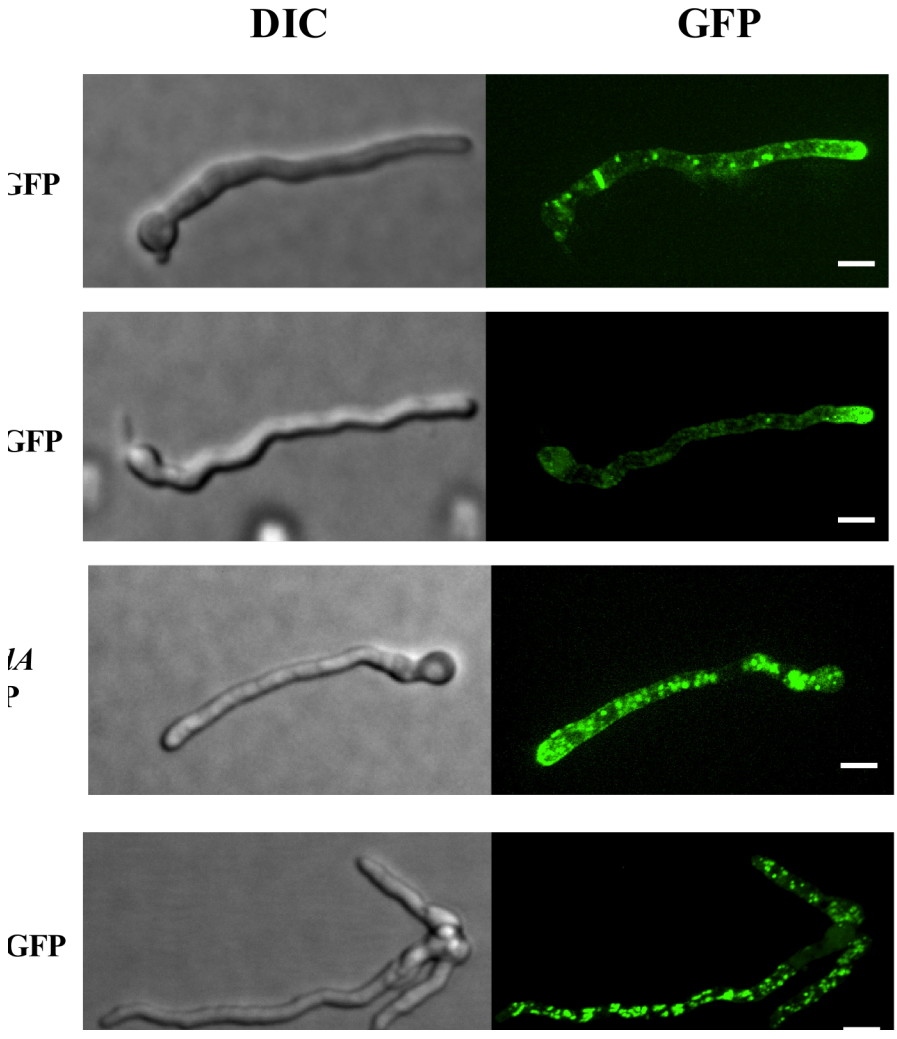
DIC
GFP
GFP
GFP
GFP

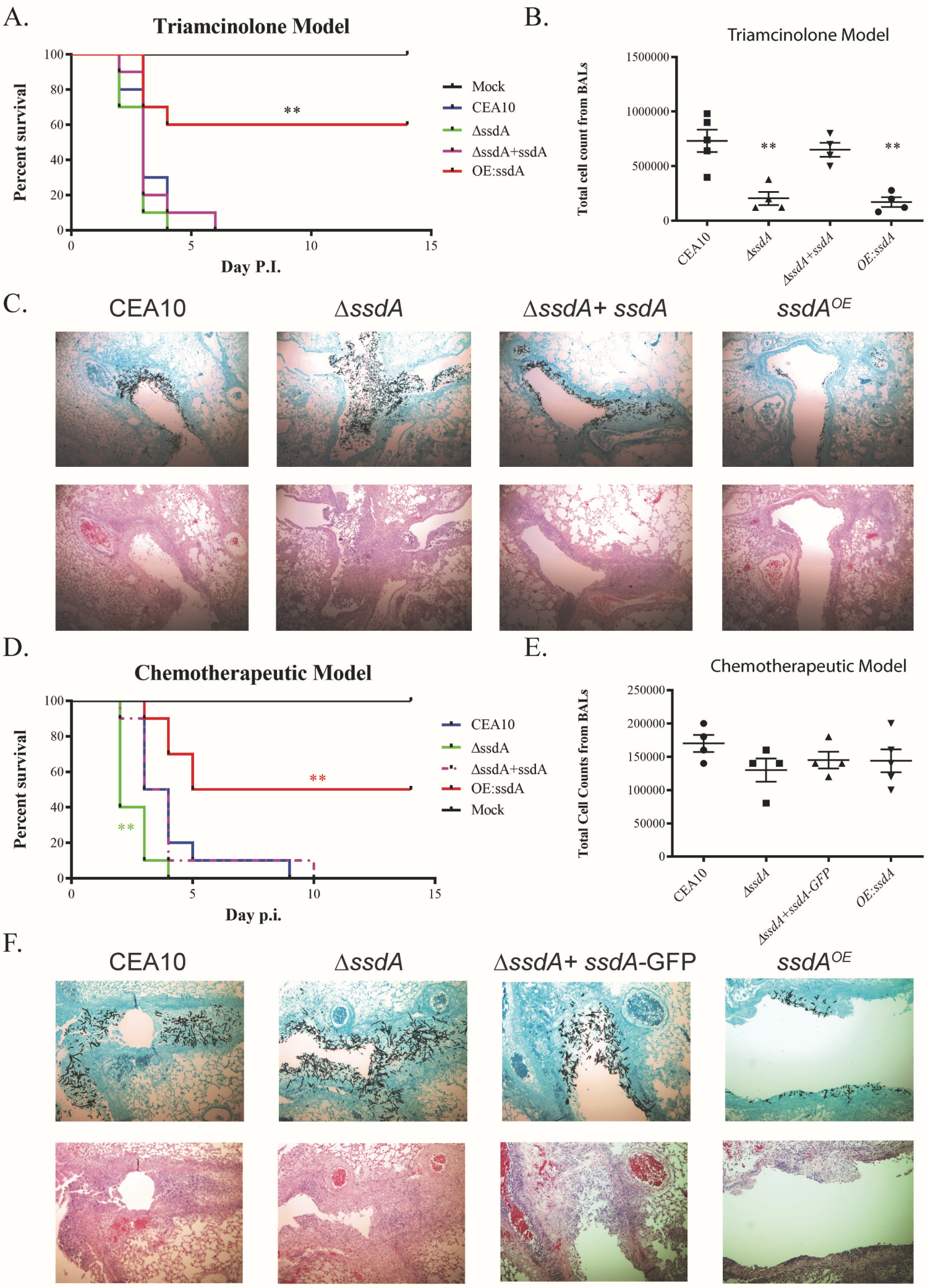
A.
Triamcinolone Model
Percent survival
Day P.I.
Mock
CEA10
ΔssdA
ΔssdA+ssdA
OE:ssdA
**
B.
Triamcinolone Model
Total cell count from BALs
CEA10
ΔssdA
ΔssdA+ssdA
OE:ssdA
C.
CEA10
ΔssdA
ΔssdA+ ssdA
ssdA^OE
D.
Chemotherapeutic Model
Percent survival
Day p.i.
CEA10
ΔssdA
ΔssdA+ssdA
OE:ssdA
Mock
E.
Chemotherapeutic Model
Total Cell Counts from BALs
CEA10
ΔssdA
ΔssdA+ssdA-GFP
OE:ssdA
F.
CEA10
ΔssdA
ΔssdA+ ssdA-GFP
ssdA^OE